Materials Characterization 128 (2017) 63–67

Contents lists available at ScienceDirect

Materials Characterization

journal homepage: www.elsevier.com/locate/matchar

Microstructural characteristics of cobalt treated by high-speed laser surface melting under high power

Jian Tu*, Kun-Feng Zhou, Zhi-Ming Zhou*, Can Huang, Hai-Long Tang

School of Materials Science and Engineering, Chongqing University of Technology, Chongqing 400054, China

ARTICLE INFO

Keywords:
Laser surface melting
EBSD
Cobalt

ABSTRACT

The microstructural evolution of cobalt (Co) treated by high-speed laser surface melting (LSM) under high power is symmetrical investigated by using electron backscatter diffraction and electron channeling contrast imaging techniques. Four distinctly different microstructural characteristics from surface to substrate are revealed in Co samples treated by LSM under high power: ε martensite plates in the elongated columnar grains for melted zone (MZ); a dual-phase microstructure (γ phase and ε phase) for heated affect zone (HAZ); deformation twins for stress affected zone (SAZ); and recrystallization microstructure for basal metal (BM). The high-speed laser treatment on Co sample shows some remarkable effects: (i) deepening the modified depth in MZ; (ii) obtaining the ultra-fine grains in HAZ; (iii) emerging one new region (SAZ). The micro-hardness reaches the highest value in HAZ due to fine grain strengthening. The metallurgical processes for the different laser-modified regions are symmetrically discussed in this paper.

1. Introduction

Cobalt (Co) alloys are widely used in medical field due to their biocompatibility, high strength, good wear and corrosion resistance [1,2]. Surface engineering is an effective technique that offers significant potential for improvement in near-surface properties [3–5], and this can also be effective for Co alloys as the biomedical devices [6]. Interestingly, laser surface melting (LSM), one surface engineering technology, is an economical treatment [7,8], and many achievements in improving near-surface performance of the engineering materials, including Fe alloys and Mg alloys, etc., have been reached by LSM treatment [9–15]. However, the attentions paid to in laser-modified Co and its alloys are still rather limited. For a better understanding the effects of LSM treatment on the macro-properties of Co and obtaining the appropriate LSM processing criterion for Co, two key influential parameters (laser processing speed and laser power) should be evaluated. The high-speed laser treatment with high power can lead to the higher cooling rate during a short residence time, thus producing a more dynamic solidification which allows for novel phase formation and more homogeneous microstructures [16]. With these in mind, the microstructural evolution in response to high-speed LSM treatment under high power is investigated by using electron channeling contrast (ECC) and electron backscatter diffraction (EBSD) techniques, aiming at preliminarily probe possible potentials of surface engineering by LSM treatment for Co and its alloys.

2. Experimental procedures

The as-received pure Co sheet (99.9%) with 2 mm thick was recrystallization sample, as shown in Fig. 1a (inverse pole figure, IPF). The recrystallized texture of Co sample is presented in Fig. 1b in term of {0001} pole figure, showing a strong basal texture with the {0001} poles largely parallel to the ND. There are differences in the standard {0001} pole figure due to the different ratios (c/a) with respect to the hexagonal materials [17]. However, it is nearly perfectly suitable for Co material since its c/a ratios (1.623) is very close to the ideal ration (1.624). The samples with dimensions of 8, 5 and 2 mm along rolling, transverse and normal directions (denoted as RD, TD and ND, respectively) were cut from the received Co sheet. Prior to pulsed laser treatment, the sample surfaces were polished with SiC paper with different grades of roughness (2400# at the final step), followed by cleaning in deionized water. Ultrasound in ethanol was used to degrease the sample surface, and LSM treatments were conducted after preparation in a short time. The RD-TD surfaces were processed along RD direction by a pulsed 600 W Nd: YAG laser device. The laser processing parameters are shown as follows, processing speed: 30 mm/s, laser emission duration time (residence time): 3 ms, pulse width: 1 ms, pulse energy: 15 J, pulse frequency: 20HZ and output power: 300 W.

After LSM treatment, the cross-sectional observations (TD-ND plane) for microstructural analyses were performed by SEM measure-

* Corresponding authors.
E-mail addresses: tujian@cqut.edu.cn (J. Tu), zhouzhiming@cqut.edu.cn (Z.-M. Zhou).

http://dx.doi.org/10.1016/j.matchar.2017.03.037
Received 7 November 2016; Received in revised form 16 March 2017; Accepted 23 March 2017
Available online 24 March 2017
1044-5803/

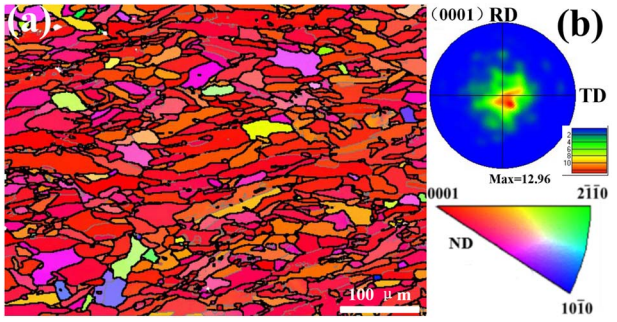

Fig. 1. EBSD maps showing a typical basal texture with the (0001) poles in recrystallized Co.

ments. Prior to SEM examinations, the specimens cut by an electrical-discharge cutting machine were mechanically ground using SiC paper (3000# at the final step) The electro-polishing was conducted at 20 V/0.5A at − 20 °C for 50 s in a solution, which is consisted of 10 ml glycerinum, 20 ml perchloric acid and 70 ml alcohol, achieving the surface quality required for SEM examination. The specimens were characterized by ECC techniques in a Zeiss Sigma HD field emission gun scanning electron microscope. In addition, step sizes used for the EBSD scanning varied from 0.08 to 0.7 μm, depending on their grain sizes. Micro-hardness distributions were examined using a HVS-1000 μ-hardness tester (Vickers indenter). Each indentation is done under a load of HV0.5 with holding time 10s. The values at ten various locations of the same depth were measured and then averaged to obtain the reliable hardness data.

3. Results and discussion

In order to comprehensively understanding the microstructural evolution in laser-modified region, the cross sectional observations (TD-ND plane) are investigated by ECC. Fig. 2a at a low magnification presents the cross-sectional overview of laser-modified Co samples at a low magnification, showing a certain penetration depth. Four distinctive zones are outlined by the dashed lines, including melted zone (MZ), heat affected zone (HAZ), stress affected zone (SAZ), and base metal (BM). Because the laser impact is confined in a certain depth, the bulk underneath acts as an infinite heat sink without any change in microstructure for BM [18]. The heat generation at the middle portion of MZ is higher than that along the circumference [19]. Thus, the heat generation at the middle portion of the modified region is higher than that at the edges, leading to a deep bowl like cross-sectional morphology, as shown in Fig. 2a. The maximal penetration depth and width within MZ are estimated to be ~400 μm and ~900 μm, respectively. Fig. 2b clearly shows three different modified regions, including MZ, HAZ and SAZ. Fig. 2c shows the transition from the heat affected region (phase transformation microstructure) to the stress affected region (deformation microstructure). One region in the molten pool exhibits "dropout" phenomenon (red arrow in Fig. 2c), which is a typical characteristic of the laser impact on metallic material [19]. In addition, the contours of several prior γ grains with irregular shape are reconstructed in HAZ (yellow arrows in Fig. 2c). After close observation in SAZ (Fig. 2c), it can be found the grains have the fiber structure, in which their directions are along the radial direction of SAZ.

Furthermore, the detailed microstructural characteristics in MZ, HAZ and SAZ are shown in Figs. 2d, e and f, respectively. The rod-shaped grains in MZ (Fig. 2d) have the size up to about tens of micrometers in width, which can be considered as the elongated columnar structure [18]. In addition, the plate-like substructure (marked by yellow arrows) is observed inside rod-shaped grains, which are formed via phase transformation during cooling process. Fig. 2e shows an abundant of plates with very fine grain size in HAZ, exhibiting four different morphology characteristics: "edge" (yellow arrow), "incomplete" (blue arrow), "island" (red arrow) and "complete" (green arrow). Their apparent shapes are just a section effect, so the "edge", "incomplete", "island" and "complete" can be considered as the same form of "incomplete" plates [20]. In addition, a plenty of deformation twins (marked by the dotted boxes) is observed in the fibrous grains in SAZ, as shown in Fig. 2f.

Fig. 3 shows the EBSD maps for cross sectional observations, including band contrast (BC) map in (a), inverse pole figure (IPF) map in (b), phase map in (c) and grain boundary (GB) map in (d). Two different zones, MZ with coarse grains and HAZ with ultra-fine grains, are separated by the dotted lines in Fig. 3a. In HAZ, the non-indexed areas are displayed in blank. IPF map shows the grains distributed rather randomly throughout MZ and HAZ (Fig. 3b), rather than the strong basal texture in BM (Fig. 1). Interestingly, the morphological characteristic in MZ likes a peacock spreading its tail feathers (Fig. 3b). In addition, the grain sizes for the elongated columnar grains in MZ decrease with the increase of the penetration depth. The different grain sizes of the elongated columnar grains along the cross sectional direction are ascribed to the varied cooling rates of diverse regions in molten pool [18]. Compared to the bottom region in MZ, the solidification time is longer in the top region. Thus, the grains in top region have enough time to grow, resulting in a larger grain size in the top region.

The phase map in Fig. 3c shows a dual-phase microstructure in MZ and HAZ, including γ phase (blue color) and ε phase (red color). In

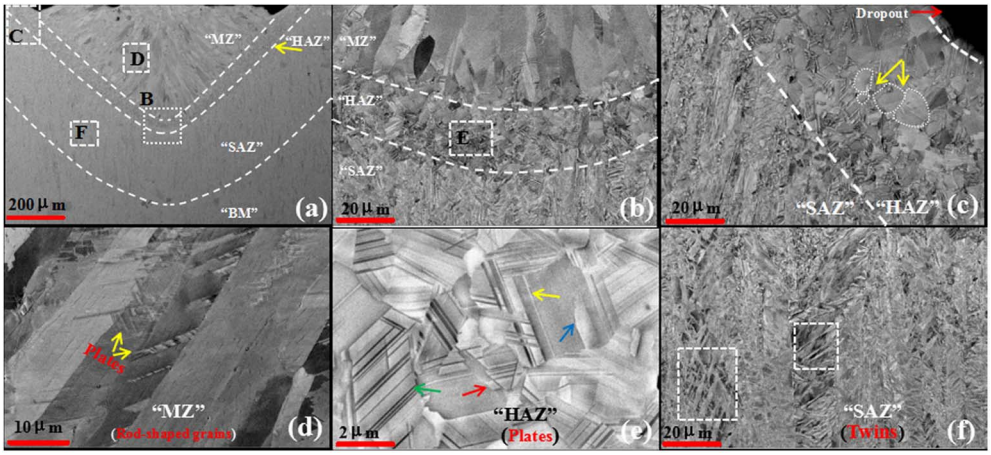

Fig. 2. Electron channeling contrast (ECC) showing microstructures of cross-sectional views at different magnification; (a) four distinctly different zones, including MZ, HAZ, SAZ and BM; (b) two transition lines: "MZ to HAZ" and "HAZ to SAZ"; (c) boundary between HAZ and SAZ; microstructural characteristics in MZ, HAZ and SAZ by ECC are shown in (d), (e) and (f), respectively. (For interpretation of the references to color in this figure, the reader is referred to the web version of this article.)